Arch. Metall. Mater. **70** (2025), 3, 1259-1266

DOI: https://doi.org/10.24425/amm.2025.154476

E. JONDA[1], M. DZIEKOŃSKA[1], M. SROKA[1*], W. PAKIEŁA[1], T. JUNG[2]

INVESTIGATION OF THE MICROSTRUCTURE AND SELECTED PROPERTIES OF LASER TREATMENT OF HVOF THERMAL SPRAYED COATINGS ONTO MAGNESIUM ALLOY SUBSTRATE

This study aimed to investigate and compare the effect of three different scanning rate laser beam heat treatments on WC-CrC-Ni coatings to identify if this method would increase the properties of coatings deposited by HVOF onto magnesium alloy substrate.

The paper presents a preliminary investigation of the microstructure and selected properties of coatings deposited by thermal spraying HVOF using commercially available WC-CrC-Ni powder and then laser treated with different values of the laser scanning rate (YLS-4000).

After laser heat treatment, the coatings were investigated regarding microstructure features and selected properties such as microhardness and dry sliding wear. The results reveal that the porosity of the laser-treated coatings had reduced in all samples while microhardness and surface roughness (Ra) strongly improved after laser treatment.

Keywords: HVOF; Laser surface treatment; AZ31 magnesium alloy; microstructure; properties

1. Introduction

Magnesium is a remarkably light metal with a density of 1.74 g/cm^3 that, unfortunately lacks strong mechanical properties [1]. Researchers have experimented with alloying magnesium with aluminium and zinc to improve its performance. These magnesium alloys maintain low density at around 1.8 g/cm^3 but exhibit significantly higher mechanical properties, particularly in specific strength. As a result, these alloys have become highly sought after for use in machine construction [2,3]. Despite these improvements, magnesium alloys still struggle with corrosion, abrasion, and erosion resistance, making them unsuitable for many industrial applications. Deposited on or changed up, the main concept is to alter the outer layer of magnesium alloys. These alloys are flammable and have a relatively low melting point (below 650°C), which makes the second approach very hopeful [4-6].

The High-Velocity Oxy-Fuel (HVOF) technology allows for producing various coatings, such as metallic, ceramic, cermet, composite, carbides, and polymers. It is commonly used to repair worn parts of machines or devices and protect against high temperatures, corrosion, and erosion [7,8]. This method offers the advantage of minimal heating to the substrate during the coating deposition process, significantly reducing any microstructural changes or deformation. An interesting characteristic of coatings deposited using this method is their adhesive joining with the substrate, as indicated by the unique wavy line formed by the mechanical jamming of plasticised powder grains during the spraying process [9-13]. Laser heat treatment offers several advantages over traditional methods. These include short processing times, low costs and precise operation [14].

Laser surface treatment aims to heat the entire coating thickness, create a metallurgical bond with a substrate, or melt the coating only to a certain depth. The advantage of this type of surface treatment is the possibility of precise control of the laser process by appropriately selected parameters [15,16].

Metal parts can have their mechanical, tribological, and chemical properties improved through laser surface treatment techniques [17]. This improvement is achieved by subjecting a thin surface layer to a quick thermal cycle, causing microstructural refinement, phase transformation, and creating alloyed or clad layers [18-20]. In the literature, some authors have concluded that laser surface heat treatment could be an excellent technique to improve durability and prevent crack growth [21].

This work attempted to use the different scanning speeds of a laser beam to modify the WC-CrC-Ni coating sprayed by HVOF and compare the microstructure and selected properties to HVOF as-sprayed coating versus laser heat treated.

[1] SILESIAN UNIVERSITY OF TECHNOLOGY,DEPARTMENT OF ENGINEERING MATERIALS AND BIOMATERIALS, 18A KONARSKIEGO STR, 44-100 GLIWICE, POLAND
[2] LUKASIEWICZ RESEARCH NETWORK – UPPER SILESIAN INSTITUTE OF TECHNOLOGY, 12 K. MIARKI STR., 44-100 GLIWICE, POLAND

* Corresponding author: marek.sroka@polsl.pl

2. Materials and methods

2.1. Substrate material

The AZ31 magnesium alloy was used as a substrate with a diameter of 100 mm and a thickness of 5 mm. The chemical composition of this material is given in TABLE 1.

TABLE 1

Chemical composition of AZ31 magnesium alloy

Element, wt.%				
Al	**Zn**	**Si**	**Mn**	**Mg**
2.5-3.5	0.6-1.4	0.0-0.3	0.0-0.2	balance

2.2. Feedstock materials

The feedstock material used in the presented studies was a commercially available WC20$Cr_3C_2$7Ni powder suitable for deposition techniques (Amperit 555.074 supplied by Höganäs). The powder was delivered as agglomerated and sintered, and its morphology was spherical (Fig. 1). The particle size of the powder was – 45 + 15 μm, and the average particle size d_{VS50} was 35.1 μm.

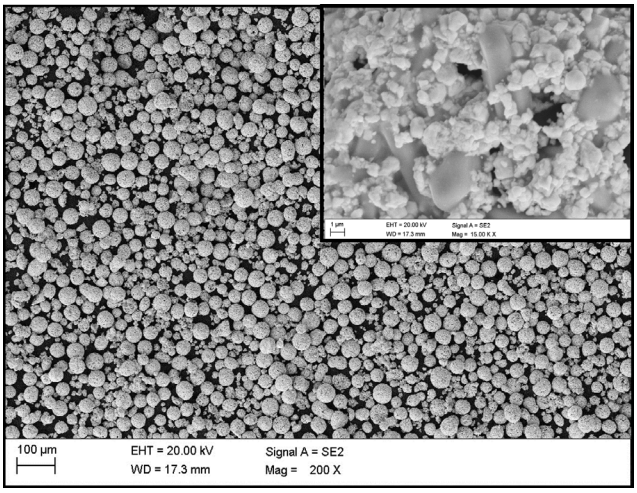

Fig. 1. The morphology of the WC-CrC-Ni powder (SEM)

2.3. Spraying process

WC-CrC-Ni cermet coatings were deposited by HVOF (High-Velocity Oxy-Fuel) method. The system C-CSJ from Thermico (CERTECH Company, Wilamowice, Poland) with a K5.2N gun was used. The kerosene and oxygen were used as the fuel media, whereas nitrogen was used as the carrier gas. The surface of the magnesium alloy substrate was pre-treated with corundum by ultrasonic sandblasting (to achieve roughness of approximately Ra = 7-8 μm). Corundum grit is F40 according to FEPA (European Producers Federation Abrasive) standard. The parameters of the HVOF process are given in TABLE 2.

TABLE 2

The process parameters of HVOF spraying

Powder	**Oxygen flow rate, l/min**	**Kerosene flow rate, l/h**	**Nitrogen flow rate, l/min**	**Powder feed rate, g/min**	**Spray distance, mm**
WC-CrC-Ni	600	40	10	25	280

2.4. Laser heat treatment procedure

The laser treatment was performed on as-sprayed WC-CrC-Ni coatings. A fibre laser FL (Fig. 2) installed on six axes was used for the surface heat treatment procedure. Ytterbium laser system YLS-4000 (IPG Photonics Corporation, Oxford, MA, USA) with a wavelength of λ = 1070 nm and a maximum laser beam power of 4000 W REIS RV30 robot -26 (Reis Robotics, Obernburg, Bavaria, Germany). Laser surface treatment was performed under argon protective gas to protect the surface of the deposited coatings. Based on a preliminary experimental study of the effect of the shielding gas, optimal parameters were selected for further studies. The parameters of laser heat treatment are shown in TABLE 3.

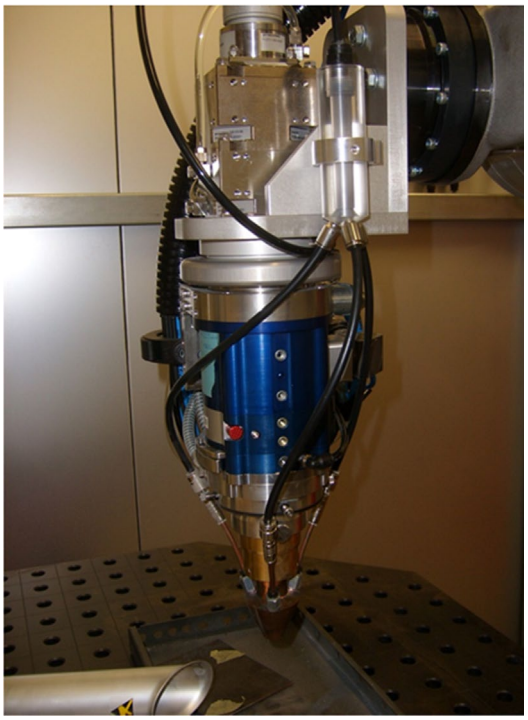

Fig. 2. The fibre laser FL Ytterbium Laser System YLS-4000

TABLE 3

Parameters of laser heat treatment

Laser beam power, kW	1
Protective gas, Bar	0.4
The share of supplied powder, g/min	15
Laser beam scanning speed, m/min	0.3
	0.4
	0.5

2.5. Characterisation of the coatings

The microstructure of sprayed and laser heat treated coatings was investigated using a scanning electron microscope (SEM, Supra 35, Zeiss, Oberkochen, Germany) to observe the polished cross-sections. These samples were prepared in a standard metallographic procedure. The chemical composition was analyzed using Energy Dispersive X-ray Spectroscopy (EDS) The porosity was assessed using the image analysis method according to the ASTM E2109-01 standard. SEM observations of polished cross-sections were made at the magnification of 1000x. All images were analysed using the open-source software ImageJ (1.50i version). X-ray diffraction determined phase analysis in a PANalytical Empyrean (Malvern, United Kingdom) diffractometer using filtered cobalt anode radiation and a Pixcel 3D detector. The qualitative phase analysis was made in the HighScore Plus software integrated with the ICDD PDF4+ database.

2.6. Surface topography and roughness

SEM also investigated the topography of the coatings. A stylus profilometer measured the surface roughness (Ra) of sprayed coatings (MarSurf PS 10, Mahr, Germany), according to the ISO 4288 standard, with Gaussian filters according to the ISO 16610-21 standard.

2.7. The microhardness, adhesion strength and dry sliding wear

The microhardness of the as-sprayed and laser heat treated coatings was investigated on the ground and polished sections by the Vickers Future-Tech FM-700 (Tokyo, Japan) according to the standard PN-EN ISO 6507-1. Measurements of changes in microhardness at a different distances from the surface were made, along lines perpendicular to specimen surfaces, and along the run face axis.

Adhesion was determined by a pull-off test and performed on a custom-built Elcometer 510 tester (Elcometer Instruments, Manchester, UK). Means and standard deviations were calculated from five measurements.

Wear resistance of the manufactured coatings was determined in the "ball-on-disc" test, according to the ASTM G99 standard with linear mode tribometer version 6.1.19 (Anton Paar, Peseux, Switzerland). The test parameters of the tests are given in TABLE 4. The counter-body was the aluminium oxide Al_2O_3 ball with a diameter of 6 mm. Before tests, the investigated samples' surface was polished to achieve a R_a value lower than 0.8 µm.

TABLE 4

The parameters of the dry sliding test

Linear speed, cm/s	Temperature, °C	Test frequency, Hz	Normal load, N	Distance, m	Counter body Al_2O_3, mm
5	20	0.4	10	50	6

3. Results and discussion

3.1. The microstructure and phase composition

A low – magnification image of the microstructure of the as-sprayed WC-CrC-Ni coating with an average thickness of 171.2 ± 19 µm is presented in Fig. 3a. It can be seen that the sprayed layer is bonded to the substrate mechanically, as indicated by the unique wavy line formed by the mechanical jamming of plasticised powder grains during the spraying process. After laser heat treatment, the greatest increase in average thickness of the coating (228.56 ± 25.17 µm) was observed after treatment with a laser beam scanning speed 0.3 m/min (Fig. 3b). This may be due to the higher density energy that causes thermal dissociation at the coating-substrate interface. Richard de Medeiros Castro et al. [22,23] came to similar conclusions. In the case of laser beam scanning speed 0.4 and 0.5 m/min, the average thickness of coatings was lower than 202.9 ± 22.5 µm and 201.6 ± 22.3 µm, respectively but still greater than thermally sprayed WC- CrC-Ni coating (Fig. 3c and d).

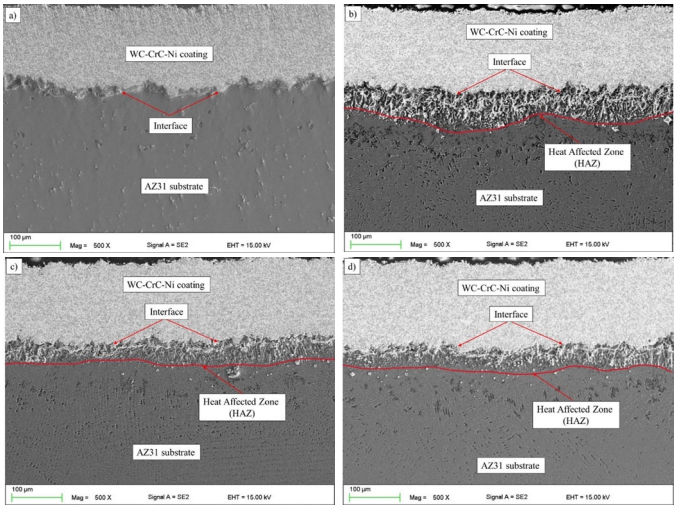

Fig. 3. The low magnification microstructure pictures of the coating: as-sprayed by HVOF method (a), and heat treated with laser beam scanning speed: 0.3 m/min (b), 0.4 m/min (c), 0.5 m/min (d)

The microstructure of the as-sprayed coating onto the magnesium alloy substrate is uniform and compact; however as shown in (Fig. 3a), some cracks (Fig. 4a) and voids (Fig. 4b) can be observed. These defects might be due to insufficient flattening of the large particles of the coating material during the short heating and high flight speed during the HVOF spraying process (Fig. 4a). The occurrence of cracks and defects in the coating could lead to delamination, which would reduce its durability [24-26]. Furthermore, Guilemany et al. reported that the presence of more micro-cracks and porosity in the coating could be the reason for increased corrosion due to electrolyte

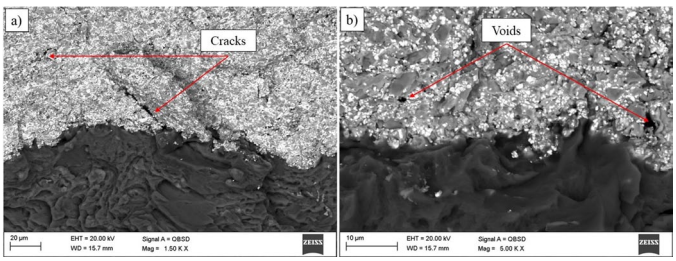

Fig. 4. The microstructure of the as–sprayed coating on to magnesium alloy substrate

infiltration at the coating layer/substrate interface [27,28]. Based on the observation of the microstructure and the point element analysis of the chemical composition (EDS), it was found that the as-sprayed coating contains unmelted or partially melted carbide particles – C (dark grey) and W (white) in a metallic Ni matrix (Fig. 5a and b). After laser heat treatment, the microstructure of the coating is more homogeneous and compact, and there are few micro-cracks and pores in it (Fig. 6a, c, e).

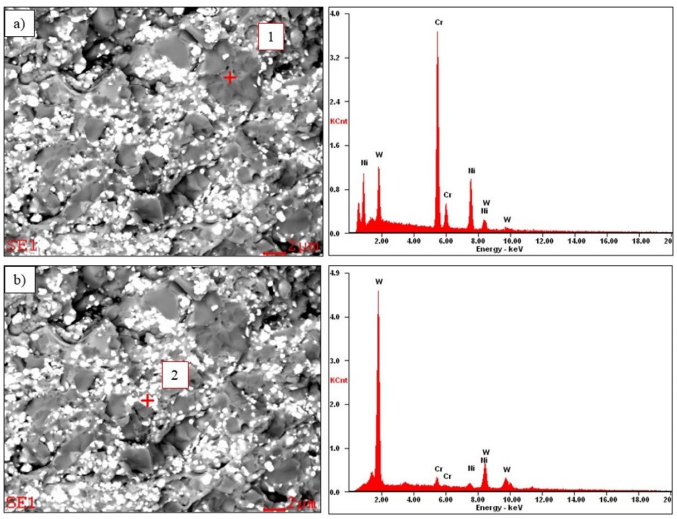

Fig. 5. The microstructure of the as-sprayed WC-CrC-Ni coating and the results of the point element analysis of the chemical composition

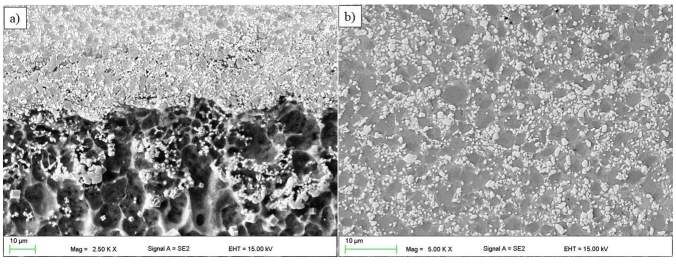

Fig. 6. SEM cross-section images of HVOF WC-CrC-Ni coating (a,c,e) and the microstructures of the laser-treated coating with partially melted and unmelted carbides (b, d, f)

In the case of laser-treated HVOF coating with different laser beam scanning speeds (0.3, 0.4, and 0.5 m/min, respectively), it could be observed that the interface between the coating and substrate is affected in all samples. The heat penetrating the coating during thermal laser treatment was probably the cause of the partial dissolution of the WC-CrC-Ni coating components and their diffusion to the substrate material. There could have been a slight dilution at the substrate-coating interface (Fig. 6a, c, e). The investigation of the coating cross-section also revealed the presence of partially melted and unmelted WC and CrC carbides in the metallic matrix (Fig. 6b, d, f). Comparable results were reported [29].

The exemplary results of the point analysis of the chemical composition (EDS) for the WC-CrC-Ni coating after heat treatment with the laser beam scanning speed of 0.4 m/min are shown in Fig. 7. As could be observed after laser treatment, the components of the HVOF sprayed WC-CrC-Ni coating were mixed with the components of the substrate material - magnesium alloy AZ31. This mixing is likely due to the diffusion of these elements, facilitated by the radiation applied to the metallic substrate [30].

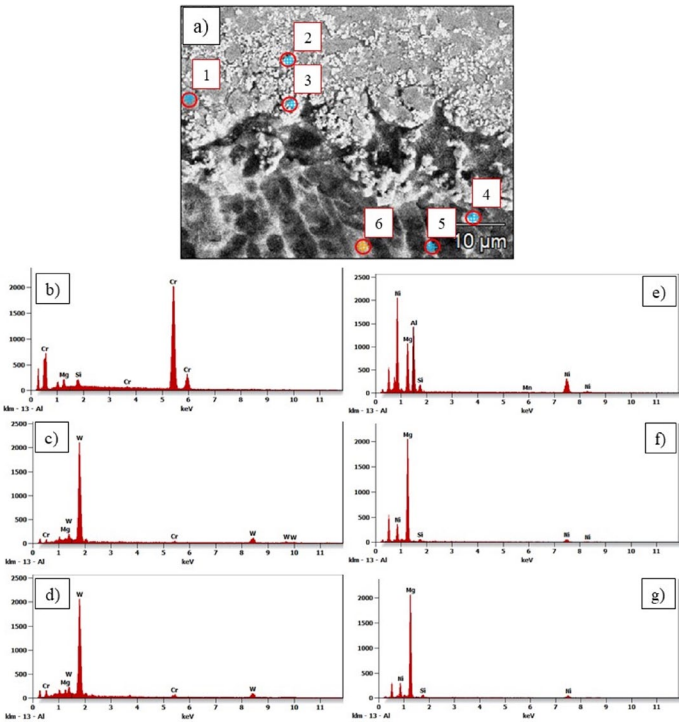

Fig. 7. The microstructure of HVOF laser treated WC-CrC-Ni coating (a), the results of chemical analysis (EDS) from points 1-6 – (b-g)

The calculated porosity value for WC-CrC-Ni deposited coating was typical for HVOF coatings, and it was equal to 3.80 ± 0.85 vol% (Fig. 4b). Mohsen Mohamed Rakhes have achieved a similar conclusion in [31,32]. On the other hand, coatings subjected to laser heat treatment are characterised by lower porosity in the range of about 3.45 ± 0.42 to 3.70 ± 0.6% vol. Reducing the scanning speed of the laser beam seems to provide enough time for porosity reduction [33].

Fig. 8 illustrates the X-ray diffraction patterns of the as-sprayed WC-CrC-Ni coating (a) and the laser treated coating with different scanning speed laser beam 0.3 m/min (b), 0.4 m/min (c) and 0.5 m/min (d).

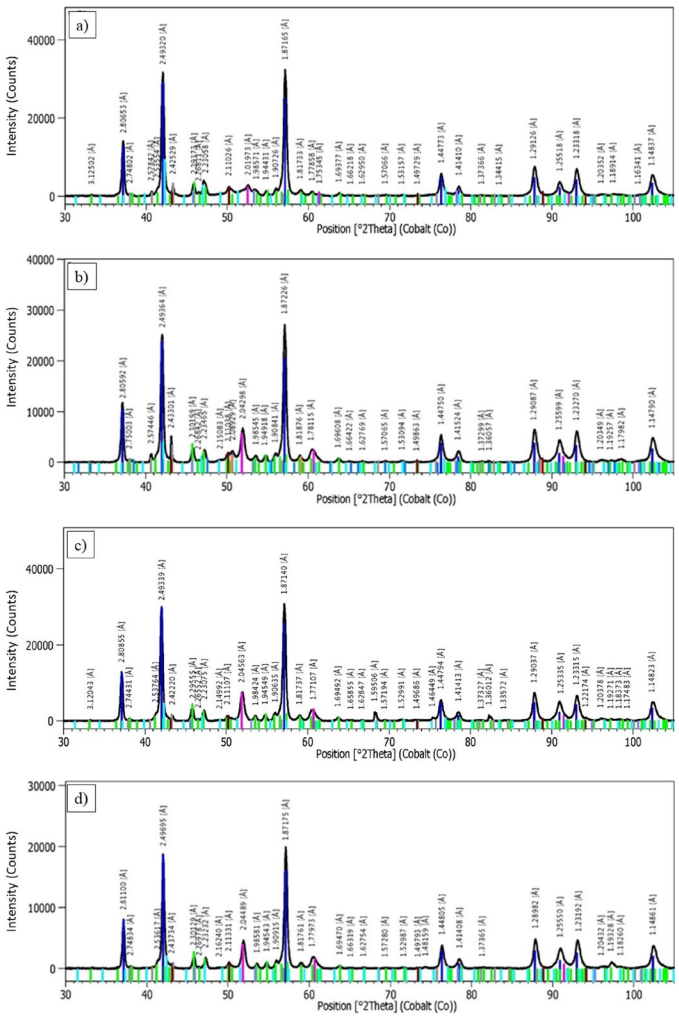

Fig. 8. XRD patterns of the as-sprayed WC-CrC-Ni coating (a) and the laser treaded coating with different scanning speed laser beam 0.3 m/min (b), 0.4 m/min (c) and 0.5 m/min (d)

The following phases were identified on each of the registered X-ray diffractograms: WC, Cr_3C_2, CrC and Ni, which are located in the WC-CrC-Ni coating sprayed with the HVOF method. In addition, trace amounts of the W_6Ni_6C ternary phase were additionally identified in a laser-treated sample at a scanning speed of 0.3 m/min. The absence of this phase in other samples (0.4 and 0.5 m/min scanning speed rate) indicates that laser processing parameters did not affect phase transformations and only created a mixture of introduced initial phases. Tungsten carbide is the dominant phase in all samples. The diffractograms also recorded phase reflections in the base derived from the AZ31 alloy: α – Mg and $Mg_{17}Al_{12}$. These reflections were likely due to the penetration of the radiation beam through the coating, which was approximately 180 µm thick [25].

3.2. Surface topography and roughness

The topography of the manufactured coating, as well as heat treated by laser, revealed irregularly shaped grains (Fig. 9a-d), which could be connected with the phenomenon that, in the flame, only the nickel matrix was melted, whereas the relatively large and hard grains of WC and CrC were not dissolved.

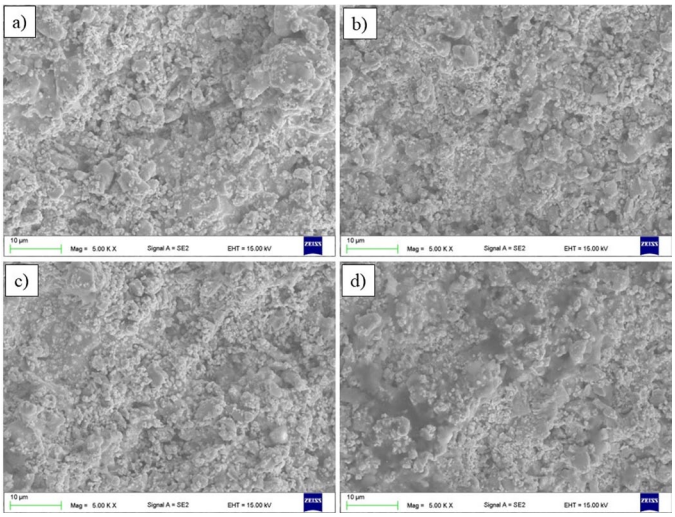

Fig. 9. The topography of the thermally sprayed coating surface (a), different scanning speed laser beam: 0.3 m/min (b), 0.4 m/min (c) and 0.5 m/min (d)

The values of average roughness (Ra – the arithmetic mean of ordinates of the roughness profile) of the WC-CrC-Ni coating before and after laser treatment are shown in TABLE 5. The results of the Ra parameter of as-sprayed coating are in the range of those reported in our previous paper [34]. When comparing values before and after laser treatment with different scanning speeds, as shown in the table, the laser treatment reduces surface roughness. The decrease in the surface roughness of the coating laser heat treated is caused by the melting or remelting of the WC-CrC-Ni powder drop on the surface of the HVOF coating as a result of the impact of the laser beam with different scanning speeds and 1 kW power [35].

TABLE 5

The average surface roughness of the WC-CrC-Ni coating in the as-sprayed condition and after laser heat treatment

Sample code	Roughness parameter Ra, µm
WC-CrC-Ni	3.91±0.40
0.3 m/min	2.76±0.31
0.4 m/min	1.62±0.25
0.5 m/min	1.10±0.12

3.3. The microhardness, adhesion strength and dry sliding wear

Fig. 10 shows the evaluation of the microhardness of the WC-CrC-Ni coating deposited by HVOF and after laser treatment with different scanning speed laser beams. A difference in the microhardness value between the as-sprayed coating and magnesium alloy substrate could be seen. The average value of the WC-CrC-Ni deposited coating was 890 ± 9 HV0.3. Com-

parable values of the microhardness were observed for coating treated with 0.3 m/min (920 ± 10 HV0.3) and 0.4 (901 ± 9 HV0.3) m/min scanning speed laser beam. A significant increase in the microhardness 1047 ± 11 HV0.3 could be seen in the laser heat treated WC-CrC-Ni coating with 0.5 m/min scanning speed laser beam [22,23].

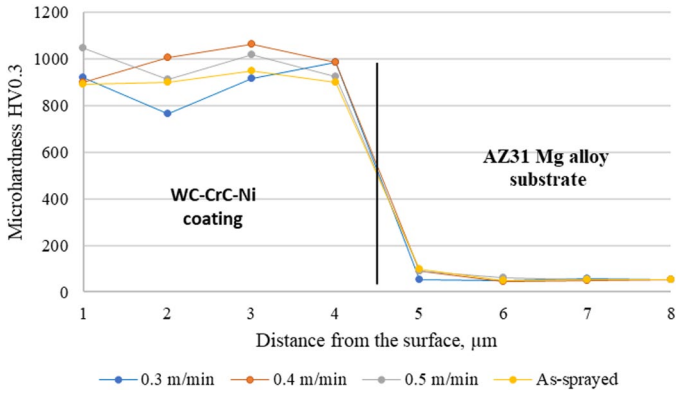

Fig. 10. Microhardness profile of as-sprayed HVOF coating and laser heat treated with different scanning speed laser beams

The adhesion of the WC-CrC-Ni coating sprayed with the HVOF method to the substrate was 43.2 ± 2.9 MPa. After thermal laser treatment, it was noticed that the adherence between the ceramic coating and the substrate material increased. The laser-treated coatings show an average adhesion strength: of 43.8 ± 3.2, 44.1 ± 3.6 and 45.3 ± 4.0 MPa for 0.3, 0.4 and 0.5 m/min scanning speed laser beams, respectively. This could be due to the diffusion of elements and forming a metallurgical bond [30]. It should be noted that the adhesion strength of HVOF-deposited coatings should generally be greater than 50 MPa. In this case, the failure occurred in the adhesive, which means that the adhesion of the coating to the magnesium alloy substrate was greater than the strength of the adhesive.

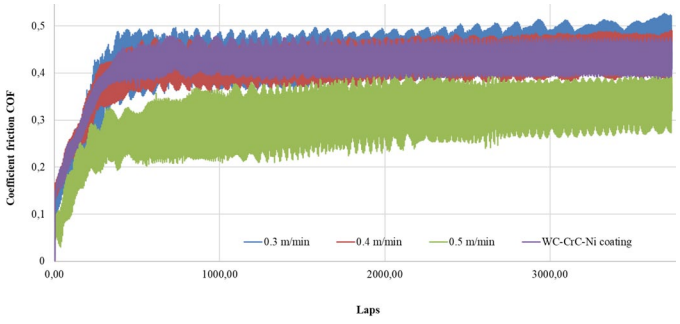

Fig. 11. The coefficient of friction of the as-sprayed HVOF coating and laser heat treated with different scanning speed laser beams

The abrasion resistance test revealed a significant impact of the laser heat treatment on the coefficient of friction recorded during the tribological test. In the case of substrate material AZ31 magnesium alloy and after laser treatment with 0.3 and 0.4 m/min scanning speed, the value of the friction coefficient was about 0.4. In contrast, the sample treated with 0.5 m/min scanning speed exhibited a lower COF of 0.3 (Fig. 11). The low coefficient of friction for the coating after laser surface treatment contributes to reduced wear. Abrasive wear resistance tests presented by G. Bolelli et al. of the WC-CoCr coating revealed a value of the friction coefficient of 0.44, while for the WC-$(W_3Cr)_2$C-Ni coating, it was over 0.6. Such high values intensify heat which promotes wear oxidation and accelerates degradation. Besides abrasion and brittle cracks, the authors also indicated oxidation as the dominant wear mechanism [36,37]. Observations of the wear tracks on the scanning microscope revealed a different nature of the existing wear mechanisms (Fig. 12). However, it should be emphasised that the basic mechanism in each case was ploughing. The characteristics of abrasive grooving can be seen on all the wear tracks.

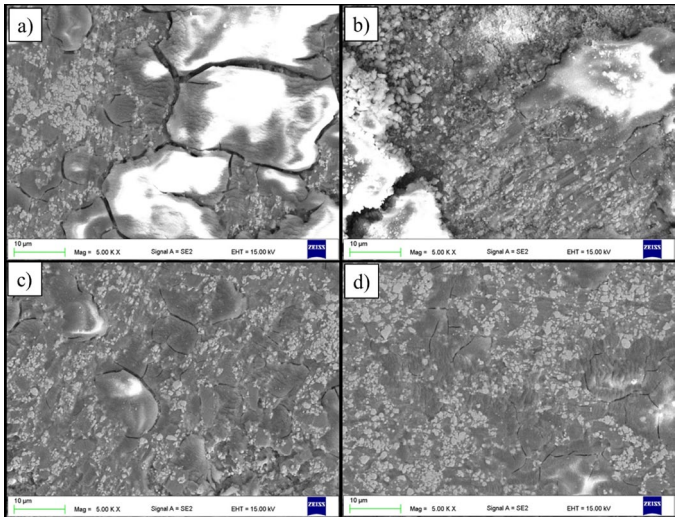

Fig. 12. The topography of the wear track of the as-sprayed HVOF coating and laser heat treated with different scanning speed laser beams

In the case of samples without laser treatment and with 0.3 m/min laser scanning speed, fatigue cracks and intense oxidation were observed (Fig. 12a). The phenomenon of oxidation is strongly correlated with a higher coefficient of friction and, thus, the amount of heat released. In addition, areas with clear traces of micro-cutting were revealed in the crater area. Traces of plastic deformation were also observed in the micro-areas. With the increase of laser scanning beam speed to 0.5 m/min, the number of fatigue cracks and oxidation traces decreased significantly. The smallest traces of fatigue wear were revealed for that sample (Fig. 12d). High coating microhardness could increase its resistance to abrasive wear. Comparable results were reported in [38]. Referring to the data in the bibliography, it could be concluded that WC-based coatings deposited by the HVOF method had good resistance to abrasive wear [39].

Measurements of the dimensions of the wear track after the abrasion resistance test allowed us to determine the rate of wear of the tested materials. After additional laser treatment with a 0.5 m/min scanning speed, the coating was characterised by the lowest wear rate. The wear rate was 8.45E-04 mm^3/s. In the case of

the sample after treatment with a speed of 0.4 m/min, the wear rate was 1.64E-03, and for 0.3 m/min, it was 1.60E-03 mm^3/s. For the untreated WC-CrC-Ni coating, the rate was 1.45E-03 mm^3/s. Based on the test results, the laser-treated coating with different scanning speeds presented good wear resistance.

4. Conclusions

Based on the investigation carried out on the WC-CrC-Ni as-sprayed by HVOF method coating and after heat treated by laser with different scanning speeds of the laser beam, the following conclusions were drawn:

1. Laser heat treatment at 0.3, 0.4 and 0.5 m/min laser speed scanning of the WC-CrC-Ni coating deposited by the HVOF method onto AZ31 magnesium alloy substrate had a positive effect on the properties of the coating because it successfully eliminated various defects in the HVOF coatings, such as porosity, cracks, and splat structure. The porosity of the coating can be prevented or significantly reduced by an appropriate, experimentally selected scanning speed and laser beam power density. Very high scanning speeds and high powers should also be avoided to avoid large penetration depths of the substrate.
2. A significant difference in microhardness was observed for the WC-CrC-Ni coating subjected to laser heat treatment at the scanning speed of the laser beam of 0.5 m/min, and it could allow the expansion of Mg alloy applications in industry.
3. As a result of laser treatment of the WC-CrC-Ni coating, its adhesion to the substrate increased, which may suggest a metallurgical bond with the substrate.
4. The abrasion resistance test revealed a significant influence of the laser heat treatment on the coefficient of friction recorded during the tribological test. Also, the investigation results have shown that the laser-treated (with different laser speed scanning rates) WC-CrC-Ni coating presented a good wear resistance.

Credit authorship contribution statement

Ewa Jonda: Conceptualization, Methodology, Investigation, Writing – Original Draft, Visualisation. **Marek Sroka**: Writing – Review & Editing. **Wojciech Pakieła**: Investigation, Writing – Review. **Tymoteusz Jung**: Investigation, **Małgorzata Dziekońska** writing – editing

Declaration of competing interest

The authors declare that they have no known competing financial interests or personal relationships that could have appeared to influence the work reported in this paper.

Founding

This research did not receive any specific grant from funding agencies in the public, commercial, or not-for-profit sectors.

REFERENCES

[1] X.W. Chen, M. Zhang, D.F. Zhang, L.P. Cai, H. Song, D.Z. Zeng, J. Alloy. Compd. 171474 (2023).
[2] M.A. Easton, M. Gibson, A. Beer, M. Barnett, Lect. N. Mobil. 17-23 (2013).
[3] F. Pan, M. Yang, X. Chen, J. Mater. Sci. Technol. **32**, 1211-1221 (2016).
[4] M. Easton, M. Gibson, S.M. Zhu, K. Yang, T. Abbott, Mater. Sci. Forum. 828-829, 3-8 (2015).
[5] T. Xu, Y. Yang, X. Peng, J. Song, F. Pan, Journal of Magnesium and Alloys **7**, 536-544 (2019).
[6] T.M. Pollock, Mater. Sci. **328**, 986-987 (2010).
[7] M. Parco, L. Zhao, J. Zwick, K. Bobzin, E. Lugscheider, Surf. Coat. Tech. **201**, 3269-3274 (2006).
[8] J.C. Tan, L. Looney, M.S.J. Hashmi, J. Mater. Process. Tech. **92-93**, 203-208 (1999).
[9] L. Pawłowski, The science and engineering of thermal spray coatings, second ed., Wiley, Chichester, England, 2008.
[10] L.-M. Berger, S. Saaro, T. Naumann, M. Kasparova, F. Zahala, J. Therm. Spray Techn. **17**, 395-403 (2008).
[11] T.S. Sidhu, S. Prakash, R.D. Agrawal, Mar. Technol. Soc. J. **39** (2), 53-64 (2005).
[12] T. Hejwowski, Characteristics of the thermal spraying process: Modern heat applied coatings resistant to abrasive and erosive wear, first ed., Lublin University of Technology, Lublin, 2013.
[13] J.R. Davis, Handbook of Thermal Spray Technology, ASM International, Materials Park, Ohio, 2004.
[14] B.S. Yilbas, S.S. Akhtar, J. Mater. Process. Tech. **212** (12), 2569-2577 (2012).
[15] M. Dharamendara, N. Jegadeeswaran, Today-Proc. **5** (11), 24937-24943 (2018).
[16] Š. Houdková, Z. Pala, E. Smazalová, M. Vostřák, Z. Česánek, Surf. Coat. Tech. **318**, 129-141 (2017).
[17] M. Von Allmen, Laser – beam interactions with materials. Physical principles and applications. Springier Series in Materials Science 2; Springer Berlin, Heidelberg, 1987.
[18] L.A. Dobrzański, E. Jonda, K. Labisz, Archives of Materials Science and Engineering **55** (2), 85-92 (2012).
[19] T. Tański, K. Labisz, Proceedings of the 2nd International Conference on Recent Trends in Structural Materials COMAT 2012 (2012).
[20] A. Lisiecki, Archives of Materials Science and Engineering **58** (2), 209-218 (2012).
[21] R.J DiMelfi, P.G Sanders, B Hunter, J.A Eastman, K.J Sawley, K.H Leong, J.M Kramer, Surf. Coat. Tech. **106 (**1), 30-43 (1998).
[22] R. de Medeiros Castro, E.I. Mercado Curi, L.F. Feltrim Inacio, A. da Silva Rocha, M. Pereira, R. Gomes Nunes Silva, A. de Souza Pinto Pereira, Surf. Coat. Tech. **427**, 127841 (2021).

[23] S.-H. Zhan, T.-Y. Cho, J.-H. Yoon, M.-X. Li, P.W. Shum, S.-C. Kwon, Mat. Sci. Eng. B **162**, 127-134 (2009).
[24] E. Jonda, M. Szala, M. Sroka, L. Łatka, M. Walczak, Appl. Surf. Sci. **608**, 155071 (2023).
[25] C. Cui, F. Ye, G. Song, Surf. Coat. Technol. **206**, 2388-2395 (2012).
[26] S.M. Nahvi, M. Jafari, Surf. Coat. Technol. **286**, 95-102 (2016).
[27] J.M. Guilemany, J. Therm. Spray Techn. **14** (3), 405-413 (2005).
[28] Z. Liu, J. Cabrero, S. Niang, Z.Y. Al-Taha, Surf. Coat. Technol. **201** (16-17), 7149-7158 (2007).
[29] M.M. Rakhes, Laser Surface Modification of HVOF Coatings for Improvement of Corrosion and Wear Performance, A thesis submitted to The University of Manchester for the degree of Doctor of Philosophy in the Faculty of Engineering and Physical Science, 2013.
[30] J. Mateos, J.M. Cuetos, R. Vijande, E. Fernandez, Tribol. Int. **34**, 345-351 (2001).
[31] K. Murugan, A. Ragupathy, V. Balasubramanian, K. Sridhar, Surf. Coat. Technol. **247**, 90-102 (2014).
[32] L.-M. Berger, S. Saaro, T. Naumann, M. Wiener, V. Weihnacht, S. Thiele, J. Suchánek, Surf. Coat. Tech. **202**, 4417-4421 (2008).
[33] S. Nemecek, L. Fidler, P. Fišerová, Physcs. Proc. **56**, 294-300 (2014).
[34] E. Jonda, L. Łatka, W. Pakieła, Materials **14**, 1594 (2021).
[35] S.H. Zhanga, J.H. Yoonb, M.X. Li, T.Y. Cho, Y.K. Joo, J.Y. Cho, Mater. Chem. Phys. **119**, 458-464 (2010).
[36] V. Matikainen, G. Bolelli, H. Koivuluoto, P. Sassatelli, L. Lusvarghi, P. Vuoristo, Wear **388-389**, 57-71 (2017).
[37] G. Bolelli, L.-M. Berger, M. Bonetti, L. Lusvarghi, Wear **309**, 96-111 (2014).
[38] G. Bolelli, L.-M. Berger, T. Börner, H. Koivuluoto, V. Matikainen, L. Lusvarghi, C. Lyphout, N. Markocsan, P. Nylén, P. Sassatelli, R. Trache, P. Vuoristo, Wear **358-359**, 32-50 (2016).
[39] A.C. Karaoglanli, M. Oge, K.M. Doleker, M. Hotamis, Surf. Coat. Tech. **318**, 299-308 (2017).